ELSEVIER

Journal of Organometallic Chemistry 637–639 (2001) 335–342

Journal of Organometallic Chemistry

www.elsevier.com/locate/jorganchem

1,1′-Ferrocenoyl–oligoprolines. A synthetic, structural and electrochemical study

Yiming Xu, Pete Saweczko, Heinz-Bernhard Kraatz *

Department of Chemistry, 110 Science Place, University of Saskatchewan, Saskatoon, Sask., Canada S7N 5C9

Received 8 January 2001; received in revised form 13 February 2001; accepted 17 February 2001

Abstract

The preparations of the eight ferrocenoyl oligopeptides, 1,1′-(Pro–OBzl)$_2$–Fc (**1**), 1,1′-(Pro–OMe)$_2$–Fc (**1a**), 1,1′-(Pro$_2$–OBzl)$_2$–Fc (**2**), 1,1′-(Pro$_3$–OBzl)$_2$–Fc (**3**), 1,1′-(Pro$_4$–OBzl)$_2$–Fc (**4**), 1-(Pro$_2$–OBzl)–1′-(OBt)–Fc (**5**), 1-(Pro$_3$–OBzl)-1′–(OBt)–Fc (**6**), 1-(Pro$_4$–OBzl)–1′-(OBt)–Fc (**7**) are described. Crystallographic studies were carried out for **1a**, showing a 1,3′-configuration of the two substitutents. The growing oligoproline chain adopts a helical polyproline-II conformation in solution. Compounds **1**–**4** exhibit reversible one-electron oxidations of the ferrocene moiety, which is influenced by the length of the oligoproline chain. With growing peptide length, the molecule becomes easier to oxidize. For the mixed OBt–ester–oligoprolines, **5**, **6** and **7**, quasi-reversible oxidations are observed at slow scan rates, which vary with the oligoproline chain length. © 2001 Elsevier Science B.V. All rights reserved.

Keywords: Ferrocene; Proline; Oligopeptide; NMR; Redox behavior; Crystal structures; Bioorganometallic

1. Introduction

We recently reported the structure–property relationship of a series of helical ferrocenoyl (Fc)–oligoprolines (Fc–P$_n$–OR, $n = 1$–4) (**I**) [1]. Elongation of the oligoproline chain to $n = 3$ caused an onset of the helical polyproline-II helix formation. This helix is stable in solution and the solid state, as judged by a combination of NMR and X-ray crystallographic studies.

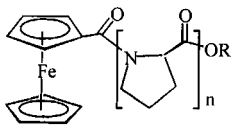

I

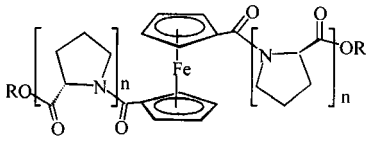

II

Interestingly, the oxidation potential of the Fc group was sensitive to the peptide substituent and its structure. Elongation of the oligoproline chain to $n = 3$ lowered the oxidation potential of the Fc group. At $n = 3$ one full helical turn polyproline-II turn was formed, and a 'final' oxidation potential of + 140 mV (vs. ferrocene/ferrocenium) for the Fc group was reached. Extending the polyproline-II chain by another proline residue to $n = 4$, caused no change in the oxidation potential. If however, the amino acid sequence of the peptide attached to the Fc group was changed to affort a peptide having a different secondary structure, the oxidation potential of the Fc group changes. It was reasoned that changes are due to electronic and not field effects, as was proposed by Gallopini and Fox for longer Aib-rich peptides [2]. For diprolinyl–phenylalanine, a β-turn was observed and the oxidation potential of the Fc group is sensitive to this change, supporting our claim that the effect on the redox potential is electronic in nature and that structural changes in the peptide are transmitted to by through-bond effects [1,3].

It would be expected that addition of a second oligoproline substitutent to the Fc moiety will cause larger changes in the redox potential. Similarly, the redox potential of other substituted ferrocene derivatives is sensitive to the number of substitutents. For example, acetylferrocene has an oxidation potential of 265 mV (vs. ferrocene/ferrocenium), whereas the oxida-

* Corresponding author. Tel.: + 1-306-966-4660; fax: + 1-306-966-4730.

E-mail address: kraatz@skyway.usask.ca (H.-B. Kraatz).

PII: S0022-328X(01)00930-5

tion potential of 1,1′-diacetylferrocene is shifted to 466 mV [4]. In analogy, we expected that for 1,1′-bis-peptide-substituted ferrocenes, we will be able to observe a larger change in the oxidation potential. For this purpose, we decided to investigate 1,1′-disubstituted ferrocenes bearing helical oligoproline substitutents (**II**). In this paper, we give a full account of syntheses, characterizations and electrochemical studies performed on these novel bis-oligoprolinoyl–ferrocene systems. We compare our results with those obtained for the monosubstituted Fc–P_n–OR ($n = 1$–4) systems. Other mono- [5] and 1,1′-disubstituted [6] ferrocenes bearing peptide substituents have been reported recently. However, in these cases, no helical peptides were attached to the ferrocene group and the design was directed towards formation of an intramolecular hydrogen bond giving rise to a β-sheet-like structure [6].

2. Experimental

2.1. General

Ferrocene dicarboxylic acid (Strem), 1-ethyl-3-(3-dimethylaminopropyl) carbodiimide (EDC), hydroxybenzotriazole (HOBt), H–Pro–OBzl·HCl, H–Pro–OMe·HCl, Boc–Pro–OH, 1,3-dicyclohexylcarbodiimide (DCC), trifluoroacetic acid (TFA) (Aldrich) were used as received. The oligoprolines Boc–Pro_n–OBzl ($n = 2$–4) were prepared as described before [7]. All solvents were dried over the appropriate drying agents and distilled under nitrogen prior to use ($CHCl_3/CaH_2$; CH_2Cl_2/CaH_2) Et_3N (Aldrich) was used without any further purification. ^{1}H- and ^{13}C-NMR spectra were recorded at 300.135 and 75.478 MHz, respectively on a Bruker AMX 300 NMR spectrometer. All chemical shifts (δ) are reported in ppm and coupling constants (J) in Hz. $CDCl_3$ (Aldrich) used for NMR spectroscopy was stored over molecular sieves (8–12 mesh; 4 Å effective pore size; Fisher). ^{1}H-NMR shift are referenced to the non-deutero impurity in $CDCl_3$ (δ 7.24) or in MeCN-d_3 and are reported relative to tetramethylsilane (δ 0.00). Assignments in the ^{1}H- and ^{13}C{^{1}H}-NMR were made using J-modulation and ^{1}H–^{1}H COSY experiments. All measurements were carried out at 293 K unless otherwise specified. Mass spectrometry was carried out on a VG Analytical 70/20 VSE instrument.

2.2. Preparation of 1,1′-Fc–(Pro–OBzl)$_2$ (1)

To a suspension of H–Pro–OBzl·HCl (0.49 g, 2.0 mmol) in CH_2Cl_2 (10 ml) was added Et_3N (0.28 ml, 2.0 mmol) with cooling to get the solution of H–Pro–OBzl in CH_2Cl_2. To a solution of 1,1′-ferrocenedicarboxylic acid (0.28 g, 1.0 mmol) in CH_2Cl_2 (15 ml) was added HOBt (0.34g, 2.2 mmol), and then it was cooled to 0 °C. After 10 min, EDC (0.42 g, 2.2 mmol) was added and it was stirred at this temperature for 30 min. The solution of H–Pro–OBzl in CH_2Cl_2 was added and the reaction mixture was stirred for 20 h. CH_2Cl_2 (40 ml) was added, the resulting solution was washed by 10% of citric acid, saturated $NaHCO_3$, H_2O, respectively, and dried over Na_2SO_4. Concentration under reduced pressure to give the crude product, which was purified by chromatography on silica gel (CH_2Cl_2:MeOH 98:2; $R_f = 0.51$) to afford 1,1′-Fc–(Pro–OBzl)$_2$ (540 mg, 83%) as an oil. Anal. Calc. for $C_{36}H_{36}N_2O_6Fe \cdot 1/2CH_2Cl_2$: C, 62.58; H, 5.25; N, 4.05. Found: C, 62.14; H, 5.44; N, 4.17%. $[\alpha]_D^{20} = -31$ (c 1.4, $CHCl_3$). IR ν_{max} (KBr) 3089, 3062, 3035, 2965, 2879, 1742, 1612 cm^{-1}. ^{1}H-NMR (δ, $CDCl_3$): 7.35 (s, 10H, Ph), 5.21 (m, 4H, OCH_2Ph), 4.86 (s, 2H, *ortho* H of Fc), 4.82 (br s, 2H, 2,2′ H of Fc), 4.65 (m, 2H, αH of Pro), 4.45 (br s, 4H, 3,3′ H of Fc), 3.88–3.74 (m, 4H, diastereotopic δH of Pro), 2.23–1.85 (m, 8H, β and γH of Pro). ^{13}C-NMR (δ, $CDCl_3$): 172.4 (Fc–C=O), 168.8 (C=O ester), 136.1, 128.7, 128.3, 128.2 (all aromatic C of Ph), 72.5 (C of Cp), 71.4 (C of Cp), 66.7 (–OCH_2Ph), 60.5 (α-CH of Pro), 48.6 (δ-CH_2 of Pro), 28.8 (CH_2 of Pro), 25.7 (CH_2 of Pro). HRMS (FAB) m/z Calc. for $C_{36}H_{37}N_2O_6Fe$ [$M^+ + 1$] 649.2001. Found 649.2002.

2.3. Preparation of 1,1′-Fc–(Pro–OMe)$_2$ (1a)

Solid DCC (0.45 g, 2.2 mmol) was added to a stirring slurry of 1,1′-ferrocenedicarboxylic acid (0.27 g, 1.0 mmol) and HOBt (0.30 g, 2.2 mmol) in CH_2Cl_2 (10 ml) at room temperature (r.t.). In a separate vessel, H–Pro–OMe·HCl (0.40 g, 2.4 mmol) was dissolved in CH_2Cl_2 (5 ml) was neutralized by Et_3N (2 ml), then transferred to the reaction vessel, which was left stirring overnight. Isolation of product from the reaction mixture was done in the same fashion as described before. Crystallization of the product from CH_2Cl_2/ether afforded **1a** as thin crystalline orange plates in 50% yield. ^{1}H-NMR (δ in ppm, $CDCl_3$): 4.86 (4H, br s, 2,2′ H Cp), 4.59 (2H, dd, $J_{HH} = 5.0$ and 8.0 Hz, CH^{α} of P_1 and $P_{1'}$), 4.47 (4H, t, $J_{HH} = 1.8$ Hz, 3,3′ H of Cp), 3.92 (2H, m, CH^{δ} P_1 and $P_{1'}$), 3.77 (8H, br s, OCH_3 and CH^{δ} P_1 and $P_{1'}$), 2.24 (2H, m, CH^{β} P_1 and $P_{1'}$), 2.13 (2H, m, CH^{β} P_1 and $P_{1'}$), 2.00 (4H, m, CH_2^{γ} P_1 and $P_{1'}$). ^{13}C{^{1}H}-NMR (δ in ppm, $CDCl_3$): 173.2 (Fc–C=O), 169.0 (C=O ester), 77.6 (C of Cp), 72.6 (C of Cp), 72.5 (C of Cp), 60.4 (α-CH of Pro), 52.3 (–OCH_3), 48.6 (δ-CH_2 of Pro), 28.9 (CH_2 of Pro), 25.8 (CH_2 of Pro). HRMS (EI): m/z Calc. for $C_{24}H_{28}N_2O_6Fe$ 496.1297 [M^+]. Found 496.1294.

2.4. Preparation of 1,1′-Fc–(Pro_2–OBzl)$_2$ (**2**) and 1,1′-Fc–(OBt)(Pro_2–OBzl) (**5**)

Boc–Pro_2–OBzl (0.40 g, 1.0 mmol) was dissolved in trifluoroacetic acid (3 ml) at 0 °C. It was allowed to warmed to r.t. and kept at this temperature for 1 h. The mixture was evaporated and the residue was dried by repeated addition of benzene and distillation to give H–Pro_2–OBzl salt. It was dissolved in CH_2Cl_2 (5 ml) and Et_3N (0.14 ml, 1.0 mmol) was added to give the solution of H–Pro_2–OBzl in CH_2Cl_2. To a solution of 1,1′-ferrocenedicarboxylic acid (0.14 g, 0.5 mmol) in CH_2Cl_2 (8 ml) was added HOBt (0.17 g, 1.1 mmol), and then it was cooled to 0 °C. After 10 min, EDC (0.21 g, 1.1 mmol) was added and it was stirred at this temperature for 30 min. The solution of H–Pro_2–OBzl in CH_2Cl_2 was added and the reaction mixture was stirred for 20 h. CH_2Cl_2 (40 ml) was added, the resulting solution was washed by 10% of citric acid, saturated $NaHCO_3$, H_2O respectively, and dried over Na_2SO_4. After filtration, the solution was evaporated to dryness to give the crude product as orange oil. Purification by chromatography on silica gel (CH_2Cl_2:MeOH 98:2) afforded solid 1,1′-Fc–(Pro_2–OBzl)$_2$ (**2**) (218 mg) and oily 1,1′-Fc–(OBt)(Pro_2–OBzl) (**5**) (224 mg).

2.5. 1,1′-Fc–(Pro_2–OBzl)$_2$ (**2**)

$R_f = 0.45$. M.p. = 80–81 °C. Anal. Calc. for $C_{46}H_{50}N_4O_8Fe{\cdot}1/2H_2O$: C, 64.86; H, 5.92; N, 6.58. Found: C, 64.74; H, 5.57; N, 6.71%. $[\alpha]_D^{20} = -109$ (*c* 1.3, $CHCl_3$). IR ν_{max} (KBr) 3062, 3035, 2973, 2875, 1742, 1658, 1608 cm^{-1}. ^{1}H-NMR (δ, $CDCl_3$): 7.31 (s, 10H, Ph), 5.18 (d, $J = 12$ Hz, 2H, diastereotopic H of OCH_2Ph), 5.05 (d, $J = 12$ Hz, 2H, diastereotopic H of OCH_2Ph), 4.88 (br s, 2H, 2,2′ H of Cp), 4.83 (br s, 2H, 2,2′ H of Cp), 4.75 (m, 2H, αH of Pro-2), 4.66 (m, 2H, αH of Pro-1), 4.47 (br s, 4H, 3,3′ H of Cp), 3.97–3.60 (m, 8H, δH of Pro-1 and Pro-2), 2.23–1.80 (m, 16H, β and γH of Pro-1 and Pro-2). ^{13}C-NMR (δ, $CDCl_3$): 172.4 (Fc–C=O), 170.9 (C=O P1/P2), 168.9 (C=O ester), 135.9, 128.7, 128.4, 128.3 (all aromatic C of Ph), 73.7 (C of Cp), 73.0 (C of Cp), 72.8 (C of Cp), 71.0 (C of Cp), 66.9 (–OCH$_2$Ph), 59.5 (α-CH of Pro-1), 59.0 (α-CH of Pro-2), 48.9 (δ-CH$_2$ of Pro-1), 46.8 (δ-CH$_2$ of Pro-2), 29.0, 28.0, 25.7, 25.1 (all CH$_2$ of Pro). HRMS (FAB) *m*/*z* Calc. for $C_{46}H_{51}N_4O_8Fe$ [M$^+$ + 1] 843.3056. Found 843.3087.

2.6. 1,1′-Fc–(OBt)(Pro_2–OBzl) (**5**)

$R_f = 0.60$. $[\alpha]_D^{20} = -42$ (*c* 0.85, $CHCl_3$). IR ν_{max} (KBr) 3073, 3030, 2959, 2877, 1781, 1743, 1690, 1652, 1609 cm^{-1}. ^{1}H-NMR ($CDCl_3$) δ 8.09 (d, $J = 8$ Hz, 1H, OBt), 7.55 (d, $J = 4$ Hz, 2H, OBt), 7.43 (m, 1H, OBt), 7.32 (s, 5H, Ph), 5.19–4.97 (m, 6H), 4.85 (m, 2H, 2,2′ H of Cp), 4.79 (m, 1H, αH of Pro), 4.65 (m, 3H, overlapping signals of αH of Pro-1 and 3,3′ H of Cp), 3.81–3.41 (m, 4H, δH of Pro), 2.16–1.94 (m, 8H, β and γH of Pro). ^{13}C-NMR (δ, $CDCl_3$): 172.4 (Fc–C=O), 170.8 (C=O P1/P2), 168.1 (C=O ester), 167.6 (C=O OBt), 143.8, 135.9, 129.1, 128.7, 128.3, 124.9, 120.6, 108.9 (all aromatic C of Ph and OBt groups), 79.0, 76.0, 73.7, 73.2, 73.0, 72.3, 72.1 (all C of Cp), 67.0 (–OCH$_2$Ph), 59.5 (α-CH of Pro), 59.0 (α-CH of Pro-2), 49.0 (δ-CH$_2$ of Pro-1), 46.8 (δ-CH$_2$ of Pro-2), 29.0, 28.0, 25.6, 25.1 (all CH$_2$ of Pro). HRMS (FAB) *m*/*z* Calc. for $C_{35}H_{34}N_5O_6Fe$ [M$^+$ + 1] 676.1859. Found 676.1860.

2.7. Preparation of 1,1′-Fc–(Pro_3–OBzl)$_2$ (**3**) and 1,1′-Fc–(OBt)(Pro_3–OBzl) (**6**)

These two compounds were prepared in a procedure analogous to that described above using Boc–Pro_3–OBzl (0.51 g, 1.02 mmol) and 1,1′-ferrocenedicarboxylic acid (140 mg, 0.51 mmol). The crude product was purified by chromatography on silica gel (CH_2Cl_2:MeOH 95:5) to afford 1,1′-Fc–(Pro_3–OBzl)$_2$ (**3**) (105 mg, 20%) and 1,1′-Fc–(OBt)(Pro_3–OBzl) (**6**) (130 mg, 33%).

2.8. 1,1′-Fc–(Pro_3–OBzl)$_2$ (**3**)

$R_f = 0.26$. M.p. = 101–104 °C. Anal. Calc. for $C_{56}H_{64}N_6O_{10}Fe{\cdot}CH_2Cl_2$: C, 59.95; H, 5.75; N, 7.49. Found: C, 60.31; H, 5.46; N, 7.39%. $[\alpha]_D^{20} = -175$ (*c* 1.0, $CHCl_3$). IR ν_{max} (KBr) 3057, 2974, 2875, 1743, 1656, 1610 cm^{-1}. ^{1}H-NMR (δ, $CDCl_3$): 7.33 (s, 10H, Ph), 5.22 (d, $J = 12$ Hz, 2H, diastereotopic H of OCH_2Ph), 5.02 (d, $J = 12$ Hz, 2H, diastereotopic H of OCH_2Ph), 4.88 (br s, 2H, 2,2′ H of Cp), 4.83 (br s, 2H, 2,2′ H of Cp), 4.81–4.74 (m, 4H, αH of Pro-2 and Pro-3), 4.56 (m, 2H, αH of Pro-1), 4.48 (s, 4H, 3,3′ H of Cp), 3.85-3.56 (m, 12H, δH of Pro), 2.24–1.90 (m, 24H, β and γH of Pro). ^{13}C-NMR (δ, $CDCl_3$): 172.2 (Fc–C=O), 170.9 (C=O), 170.7 (C=O), 168.8 (C=O ester), 135.8, 128.7, 128.5, 128.4 (all aromatic C of Ph), 72.7 (C of Cp), 71.1 (C of Cp), 67.0 (–OCH$_2$Ph), 59.6 (α-CH of Pro-1), 58.9 (α-CH of Pro), 58.0 (α-CH of Pro), 48.9 (δ-CH$_2$ of Pro-1), 47.1, 46.8 (all δ-CH$_2$ of Pro), 28.9, 28.1, 27.9, 25.7, 25.0, 24.9 (all CH$_2$ of Pro). HRMS (FAB) *m*/*z* Calc. for $C_{56}H_{65}N_6O_{10}Fe$ [M$^+$ + 1] 1037.4112. Found 1037.4122.

2.9. 1,1′-Fc–(OBt)(Pro_3–OBzl) (**6**)

$R_f = 0.44$. M.p. = 57–59 °C. Anal. Calc. for $C_{40}H_{40}N_6O_7Fe{\cdot}1/2H_2O$: C, 61.46; H, 5.16; N, 10.75. Found: C, 61.49; H, 4.98; N, 10.54%. $[\alpha]_D^{20} = -32$ (*c* 1.0, $CHCl_3$). IR ν_{max} (KBr) 3078, 3030, 2974, 2877, 1780, 1743, 1691, 1650, 1608 cm^{-1}. ^{1}H-NMR (δ, $CDCl_3$): 8.06 (d, $J = 8$ Hz, 1H, OBt), 7.46 (d, $J = 8$ Hz,

1H, OBt), 7.53 (m, 1H, OBt), 7.41 (m, 1H, OBt), 7.30 (m, 5H, Ph), 5.19–4.93 (m, 6H, overlapping signals of αH of Pro and 2,2′ H of Cp), 4.80 (m, 3H), 4.57 (m, 4H, overlapping signals of αH of Pro and 3,3′ H of Cp), 3.92–3.44 (m, 6H, δH of Pro), 1.97–1.77 (m, 12H β and γH of Pro). ^{13}C-NMR (δ, $CDCl_3$): 172.2 (Fc–C=O), 170.9 (C=O), 170.5 (C=O), 168.1 (C=O ester), 167.5 (C=O OBt), 143.7, 135.9, 129.1, 128.9, 128.7, 128.5, 128.4, 125.0, 120.6, 109.1 (all aromatic C of Ph and OBt), 79.1, 75.8, 75.4, 73.8, 73.1, 73.0, 72.3, 72.1 (all C of Cp), 67.0 (–O*C*H$_2$Ph), 59.6 (α-*C*H of Pro-1), 58.9, 58.0 (both α-*C*H of Pro), 49.0, 47.1, 46.7 (all δ-*C*H$_2$ of Pro), 29.0, 28.0, 25.7, 25.0, 24.8 (all *C*H$_2$ of Pro). HRMS (FAB) m/z Calc. for $C_{40}H_{41}N_6O_7Fe$ [$M^+ + 1$] 773.2386. Found 773.2390.

2.10. Preparation of 1,1′-Fc–(Pro$_4$–OBzl)$_2$ (4) and 1,1′-Fc–(OBt)(Pro$_4$–OBzl) (7)

These two compounds were prepared in a procedure analogous to that described above using Boc–Pro$_4$–OBzl (0.43 g, 0.57 mmol) and 1,1′-ferrocenedicarboxylic acid (78 mg, 0.29 mmol). The crude product was purified by chromatography on silica gel (CH_2Cl_2:MeOH 93:7) to afford the desired products 1,1′-Fc–(Pro$_4$–OBzl)$_2$ (**4**) (51 mg, 15%) and 1,1′-Fc–(OBt)(Pro$_4$–OBzl) (**7**) (66 mg, 27%).

2.11. 1,1′-Fc-(Pro$_4$–OBzl)$_2$ (4)

$R_f = 0.16$. M.p. = 117–118 °C. Anal. Calc. for $C_{66}H_{78}N_8O_{12}Fe{\cdot}3H_2O$: C, 61.20; H, 6.07; N, 8.65. Found: C, 61.33; H, 6.48; N, 8.41%. $[\alpha]_D^{20} = -181$ (*c* 1.0, $CHCl_3$). IR ν_{max} (KBr) 3051, 2974, 2875, 1743, 1649, 1604 cm^{-1}. ^{1}H-NMR (δ, $CDCl_3$): 7.32 (s, 10H, Ph), 5.20 (d, $J = 12$ Hz, 2H, diastereotopic H of OC*H*$_2$Ph), 4.99 (d, $J = 12$ Hz, 2H, diastereotopic H of OC*H*$_2$Ph), 4.86 (br s, 2H, 2, 2′ H of Fc), 4.82 (br s, 2H, 2,2′ H of Fc), 4.80–4.68 (m, 6H, αH of Pro-2, Pro-3, and Pro-4), 4.59 (m, 2H, αH of Pro-1), 4.47 (br s, 4H, 3,3′ H of Fc), 3.82–3.57 (m, 16H, δH of Pro), 2.16–1.85 (m, 32H, β and γH of Pro). ^{13}C-NMR (δ, $CDCl_3$): 172.2 (Fc–C=O), 170.7 (C=O), 170.6 (C=O), 168.9 (C=O ester), 135.8, 128.7, 128.4 (all aromatic C of Ph), 72.8, 71.0 (both C of Cp), 67.1 (–O*C*H$_2$Ph), 59.6, 59.0, 58.2, 58.0 (α-*C*H of Pro), 49.0, 47.3, 47.1, 46.7 (all δ-*C*H$_2$ of Pro), 28.9, 28.2, 28.0, 25.8, 25.0, 24.8 (all *C*H$_2$ of Pro). HRMS (FAB) m/z Calc. for $C_{66}H_{79}N_8O_{12}Fe$ [$M^+ + 1$] 1231.5167. Found 1231.5163.

2.12. 1,1′-Fc–(OBt)(Pro$_4$–OBzl) (7)

$R_f = 0.40$. M.p. = 85–88 °C, $[\alpha]_D^{20} = -16$ (*c* 1.0, $CHCl_3$). IR ν_{max} (KBr) 3085, 2972, 2875, 1780, 1743, 1649, 1609 cm^{-1}. ^{1}H-NMR (δ, $CDCl_3$): 8.08 (d, $J = 8$ Hz, 1H, OBt), 7.58 (m, 2H, OBt), 7.43 (m, 1H, OBt), 7.31 (s, 5H, Ph), 5.18–4.95 (m, 6H), 4.83 (m, 3H), 4.62 (m, 2H), 4.57 (m, 2H), 3.90–3.52 (m, 8H, δH of Pro), 2.18–1.89 (m, 16H, β and γH of Pro). ^{13}C-NMR (δ, $CDCl_3$): 172.2 (Fc–C=O), 170.7 (C=O), 170.5 (C=O), 168.1 (C=O ester), 167.4 (C=O OBt), 143.7, 135.8, 129.1, 128.8, 128.4, 125.0, 120.6, 109.0 (all aromatic C of Ph and OBt), 79.2, 75.8, 75.6, 73.8, 73.0, 72.3 (all C of Cp), 67.1 (–O*C*H$_2$Ph), 59.6, 58.9, 58.0 (all (α-*C*H of Pro), 49.0, 47.3, 47.0, 46.7 (all δ-*C*H$_2$ of Pro), 28.9, 28.0, 25.7, 25.0, 24.8 (all *C*H$_2$ of Pro),. HRMS (FAB) m/z Calc. for $C_{45}H_{48}N_7O_8Fe$ [$M^+ + 1$] 870.2914. Found 870.2918.

2.13. Electrochemical studies

All electrochemical experiments were carried out using a CV-50W voltammetric analyzer (BAS) at r.t. (23 °C). No special precautions were taken to exclude oxygen. All experiments were carried out in acetonitrile, which was dried over CaH_2 and distilled prior to use. Tetrabutylammonium perchlorate (TBAP) was used as supporting electrolyte (0.1 M). For the cyclic voltammetry studies a glassy carbon-working electrode (BAS, diameter 2 mm) and a platinum wire counter electrode were used. The glassy carbon-working electrode was polished with 3 μm followed by 1 μm, then 0.5 μm alumina prior to use to remove any surface contaminants. The reference electrode was a Ag | AgCl electrode (BAS). IR compensation was applied. Backgrounds of the solvent containing 0.1 M TBAP were collected before each set of experiments and then subtracted from the spectra.

2.14. X-ray crystallography

Very thin plates of **1a** were obtained from CH_2Cl_2 by slow evaporation at room temperature and mounted on a glass fiber using epoxy resin. Despite the poor quality of the crystal, we collected a data set using a Siemens SMART CCD diffractometer Mo–K_α radiation (graphite monochromated) using ω-scans. The structure of **1a** was solved by direct methods using the SHELXTL [8]. All non-hydrogen atoms were refined anisotropically using full-matrix least-squares to give the final R values of $R = 0.0924$, $R_w = 0.2158$ for 3271 observed reflections ($I > 2\sigma(I)$). All crystallographic details have been summarized in Table 1.

3. Results and discussion

These synthetic procedures discussed in this paper are summarized in Scheme 1.

Oligoprolines (Boc–Pro$_n$–OBzl) were synthesized from commercially available Boc–Pro–OH and H–Pro–OBzl·HCl in CH_2Cl_2 solution following the pub-

Table 1
Crystal data and structure refinement for **1a**

Empirical formula	$C_{24}H_{20}FeN_2O_4$
Formula weight	456.27
Temperature (K)	193(2)
Wavelength (Å)	0.71073
Crystal system	Orthorhombic
Space group	$P2_12_12_1$
Unit cell dimensions	
a (Å)	8.918(3)
b (Å)	11.858(3)
c (Å)	21.403(6)
V (Å^3)	2263.4(11)
Z	4
D_{calc} (g m^{-3})	1.339
Absorption coefficient (mm^{-1})	0.698
$F(000)$	944
Crystal size (mm^3)	$0.30\times0.25\times0.05$
θ Range for data collection (°)	1.90 to 23.33
Limiting indices	$-9<h<9$, $-13<k<13$, $-23<l<23$
Reflections collected	17 348
Independent reflections	3271 ($R_{int}=0.2013$)
Data/restraints/parameters	3271/0/314
Goodness-of-fit (F^2)	0.995
Final R indices [$I>2\sigma(I)$]	$R_1=0.0924$, $wR_2=0.2158$
R indices (all data)	$R_1=0.1356$, $wR_2=0.2458$
Abs. structure parameter	−0.04(6)
Largest difference peak and hole (e Å^{-3})	1.596 and −0.946

lished procedures [7]. While coupling of H–Pro–OBzl with 1,1′-ferrocenedicarboxylic acid in CH_2Cl_2 using hydroxybenzotriazole (HOBt) and 1-ethyl-3-(3-dimethylaminopropyl) carbodiimide (EDC) resulted bis-prolinoyl–ferrocene (**1**) in good yields. The corresponding reaction with diproline-, triproline- and tetraproline-benzylesters resulted in the formation of two classes of products: the desired bis-oligoprolinoyl ferrocene derivatives (**2**–**4**) and 1-oligoprolinoyl–1′-OBt–ferrocene derivatives (**5**–**7**). We were excited to be able to synthesize these by-products as they provide a simple access to asymmetrically substituted ferrocenoyl derivatives. Compounds **5**–**7** are air and moisture stable in common solvent and are readily separated from the bis-oligoprolinoyl–ferrocenes (**2**–**4**) by chromatography on silica gel. All compounds were fully characterized by ^{1}H- and ^{13}C-NMR spectroscopy, HRMS, optical rotation and elemental analysis.

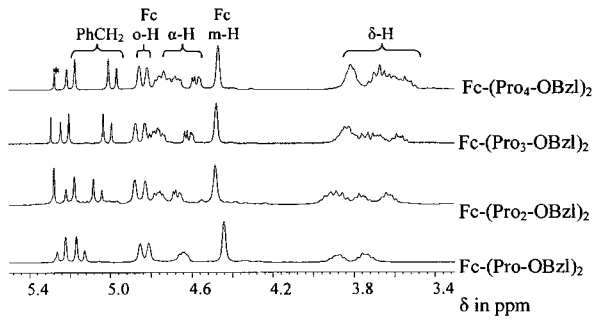

Fig. 1. Partial ^{1}H-NMR of 1,1′-Fc–(Pro$_n$–OBzl)$_2$ ($n=1$–4) (**1**–**4**) in the region of 5.50–3.30 ppm.

In the NMR spectra (^{1}H and ^{13}C{^{1}H}) of **1**–**4**, both Cp–P$_n$–OMe ($n=1$, 2) portions are magnetically equivalent due to a C_2 symmetry axis, and therefore only one set of signals corresponding to both oligoproline portions of the molecule is observed. Fig. 1 shows a stackplot of partial ^{1}H-NMR spectra for compounds **1**–**4** in the region from δ 5.5–3.3.

For **1**–**4**, the 3,3′-protons of the Cp rings are magnetically equivalent and give rise to a signal near δ 4.48. The two diastereotopic 2,2′-protons of the Cp, being closer to the asymmetric center on the proline ring, are observed as two individual signals in narrow shift regions around δ 4.86 and 4.80, respectively. Importantly, each type of proton, such as the α-proton or the δ-proton of each individual proline ring, gives rise to a signal in a characteristic region of the ^{1}H-NMR. The α-protons of all proline residues appear as multiplets between 2,2′- and 3,3′-proton resonances of the two Cp rings. Importantly, the α-protons of the proline residues for all compounds **1**–**7** are in a region of the spectrum characteristic for the peptide chain being in the helical polyproline-II conformation with all proline linkages being *trans* [1]. It is interesting to point out that for all systems **1**–**7**, the α-proton of the proline residue which is attached to the Fc group is observed at δ 4.64, slightly upfield from the other α-protons that are part

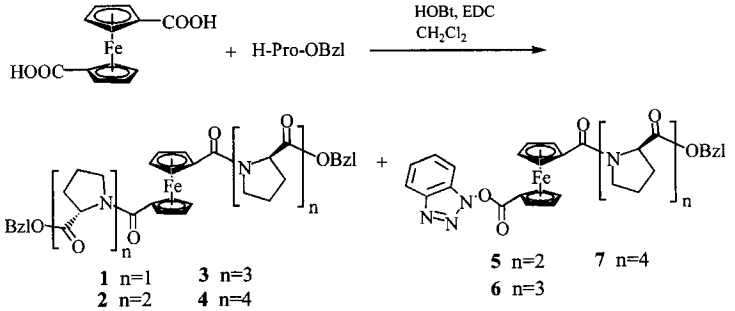

Scheme 1. Syntheses of 1,1′-di(oligoprolinoyl)–ferrocenes (**1**–**4**) and 1-oligoprolinoyl–1′-benzotriazole ester–ferrocenes (**5**–**7**).

of the oligoproline chain, which are observed around δ 4.80. As the proline chain grows, the signal of the α-H of additional proline residues overlaps with those signals at δ 4.80. The two diastereotopic δ-H of all proline rings appear as multiplets in the region δ 3.92 and δ 3.66. The signals arising from the remaining diastereotopic protons of the methylene groups of all proline rings, appear as multiplets around δ 2.0. The ^{13}C-NMR of **1**–**4** exhibits a single set of resonances for both oligoproline residues at the two Cp rings, as expected for a molecule having a C_2 axis. For **1**, two carbonyl resonances at δ 172.4 (Fc–amide) and δ 168.8 (benzylester) are observed. For **2**–**4**, additional amide signals appear between these two resonances. Signals for the α-, δ-, β- and γ-carbon atoms of the proline residues are in characteristic regions [1]. All α-carbons are observed near δ 60, whereas δ-carbon signals are observed around δ 47. β- and γ-carbon atoms are at significantly higher field (δ 28–24). The NMR spectra of the unsymmetrically substituted systems **5**–**7** are much more complex due to the loss of symmetry. Thus, the ^{13}C-NMR spectrum shows ten signals for the ten inequivalent carbon atoms of the two Cp rings. Interestingly, the signals due to the oligoproline residues are not influenced by the presence of the –OBt residue.

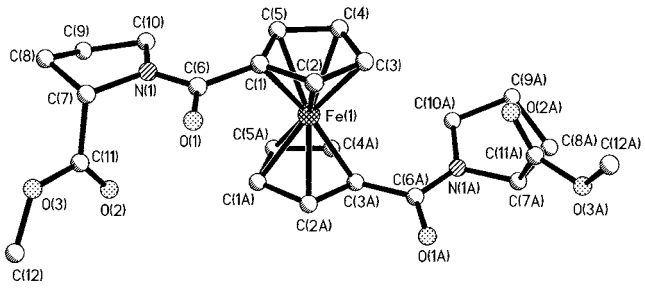

Fig. 2. Molecular structure of **1a**, showing the 1,3′-conformation of the two Cp rings minimizing the steric interaction between the two prolinoyl–methylester residues. Hydrogen atoms have been omitted for clarity.

Table 2
Selected bond lengths (Å) and bond angles (°) for **1a**

Bond lengths			
Fe(1)–$C_{Cp\ ave}$	2.049(11)	Fe(1)–$C_{Cpa\ ave}$	2.040(11)
O(1)–C(6)	1.219(11)	O(1a)–C(6a)	1.227(11)
O(2)–C(11)	1.182(13)	O(2a)–C(11a)	1.204(14)
O(3)–C(11)	1.331(13)	O(3a)–C(11a)	1.312(13)
O(3)–C(12)	1.460(15)	O(3a)–C(12a)	1.445(17)
N(1)–C(6)	1.345(13)	N(1a)–C(6a)	1.364(13)
N(1)–C(7)	1.476(13)	N(1a)–C(7a)	1.495(13)
N(1)–C(10)	1.477(13)	N(1a)–C(10a)	1.458(13)
C(6)–C(1)	1.515(14)	C(6a)–C(3a)	1.481(14)
Bond angles			
C(6)–N(1)–C(10)	129.2(9)	C(6a)–N(1a)–C(10a)	128.9(9)
C(6)–N(1)–C(7)	117.9(8)	C(6a)–N(1a)–C(7a)	116.8(8)
C(7)–N(1)–C(10)	112.7(8)	C(7a)–N(1a)–C(10a)	113.5(8)
O(1)–C(6)–N(1)	120.5(10)	O(1a)–C(6a)–N(1a)	120.1(9)

Table 3
Results of the electrochemical studies of 1,1′-Fc–(Pro$_n$–OBzl)$_2$ (n = 1–4) (**1**–**4**) and 1,1′-Fc–(OBt)(Pro$_n$–OBzl) (n = 2–4) (**5**–**7**)

Compound		$E_{1/2}$ [a]	ΔE_p	i_a/i_c
1,1′-Fc–(Pro–OBzl)$_2$	**1**	320 ± 2	61	0.99
1,1′-Fc–(Pro$_2$–OBzl)$_2$	**2**	285 ± 2	66	0.89
1,1′-Fc–(Pro$_3$–OBzl)$_2$	**3**	275 ± 2	61	1
1,1′-Fc–(Pro$_4$–OBzl)$_2$	**4**	275 ± 3	64	0.91
1,1′-Fc–(OBt)(Pro$_2$–OBzl)	**5**	570 ± 20 [b]		
1,1′-Fc–(OBt)(Pro$_3$–OBzl)	**6**	545 ± 4 [c]	>150	
1,1′-Fc–(OBt)(Pro$_4$–OBzl)	**7**	562 ± 5 [c]	>150	

Halfwave potentials ($E_{1/2}$) and peak separation (ΔE_p) are in mV. All potentials are referenced to an internal ferrocene/ferrocenium redox couple (430 mV vs. Ag | AgCl).

[a] 0.1 M TBAP in dry MeCN using a glassy carbon working electrode, Pt counter electrode and a Ag | AgCl references electrode.

[b] Irreversible oxidation at scan rates up to 2000 mV s^{-1}.

[c] Measured at a scan rate of 1000 mV s^{-1}.

Compound **1** exhibits a two IR absorptions for the ester C=O and the amide C=O vibrations at 1742 and 1612 cm^{-1}, respectively. For **2**–**4** an additional band at about 1650 cm^{-1} appears and can be assigned to the additional amide bonds which are present in these molecules. For the OBt–oligoprolinoyl systems **5**–**7**, up to two new bands are observed: a higher energy ester band for the OBt–ester C=O stretch at 1780 cm^{-1} and a new amide band at 1690 cm^{-1}.

The structure of a methyl analogue of **1** (**1a**) is shown in Fig. 2. Selected bond distances and angles are given in Table 2.

The compound exhibits a 1,3′ conformation of the substituents. This conformation minimizes steric interactions of the substituents and is typical for bis-ring substituted ferrocenes. The 1,1′-conformation is usually found only for systems that exhibit strong intramolecular hydrogen bonding [3,6]. The Fe–Cp(centroid) distance is 2.049(11) Å. The carbonyl distances C(1)–O(6) and C(1A)–O(6A) are 1.219(11) and 1.227(11) Å, respectively. The Cp-ring–amide carbon distances C(1)–C(6) and C(3A)–C(6A) distances are typical for ferrocenoyl systems. The distances and angles within the proline substitutents show no distortion and compare well with those reported for other proline containing oligopeptides.

Next, we proceeded to investigate the redox chemistry of the disubstituted ferrocenoyl–oligoprolines and OBt–esters **1**–**7** by cyclic voltammetry in acetonitrile using ferrocene as an internal standard (430 mV vs. Ag | AgCl). The redox behaviors of these systems are significantly influenced by the nature of the substituents. For **1**–**4**, fully reversible one-electron oxidations [9] were observed at 100 mV s^{-1} with the ratio of anodic to cathodic peak currents close to unity (see Table 3). The cyclic voltammogram for **1** is shown in

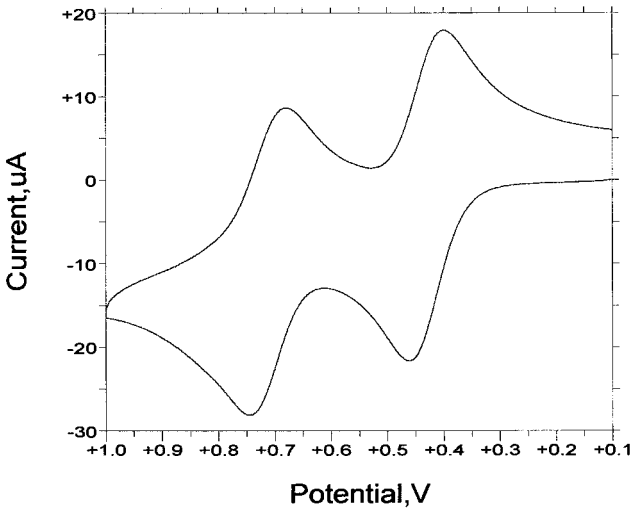

Fig. 3. Cyclic voltammogram of **2** in acetonitrile. The halfwave potential $E_{1/2}$ of **2** at 285 mV is referenced to internal ferrocene/ferrocenium ($E_{1/2} = 430$ mV vs. Ag | AgCl).

Fig. 3. As for the monosubstituted Fc–oligoprolines, the redox properties of the Fc moiety are dependent on the chainlength and structure of the oligoproline substitutent [1]. With growing oligoproline chain length, the molecule becomes easier to oxidize. The redox potentials for the di-oligoproline substituted systems are about double that of the corresponding monosubstituted Fc–Pro_n–OBzl systems. The oxidation potential for the monoproline system **1** was observed at 320 ± 2 mV (vs. ferrocene/ferrocenium). Elongation of the oligoproline chain by one or more proline residues resulted in shifts of the redox potential to 280 ± 2 mV for **2** and 275 ± 2 mV for **3**. After three proline residues, which are required for a full helical turn of the peptide, resulting in the formation of a polyproline-II helix, no further changes of the redox potential were observed. This behavior is in line with results obtained for monosubstituted Fc–oligoprolines and it provides additional support that the redox properties of the ferrocenoyl moiety is sensitive to the structural properties of the oligopeptide chain. Effects caused by the dipole [2] of the peptide chain are of no consequence. Again, effects due to the dipole of the peptide chain are not important. The Fc moiety is at the center of two peptide chains with dipoles pointing away from the Fc group (for possible 1,1′, 1,2′, and 1,3′ conformations in solution). Thus, the Fc moiety is at the positive end of the dipole, yet increasing the oligoproline chain leads to a relative stabilization of the $Fc^{+\cdot}$. This is the second example of this type of behavior and is in contrast to results by Fox on dipolar effects in helical Aib-rich peptides. This suggests that factors other than electric field effects caused by the peptide's dipole are influencing the redox potentials in Fc–Pro_n–OBzl and 1,1′-$(Pro_n)_2$–Fc systems.

For **5**–**7**, only quasi-reversible oxidations [9] are observed at slow scan rates (100 mV s^{-1}), suggesting an EC mechanism, in which after oxidation, the Fc^+-compound undergoes a chemical reaction. We propose that this reaction involves the C–O bond of the OBt-active ester. Oxidation of the complex may result in cleavage of the C–O bond and formation of a benzotriazolyl radical. For **6** and **7**, an increase in the scan rate causes the oxidation to become more reversible and on the reverse scan a signal for the reduction of $\mathbf{6}^+$ to **6** is observed. Fig. 3 shows the CV curves of **6** at various scan rates. For **6**, this quasi-reversible oxidation is observed at 545 ± 4 mV (vs. Fc/Fc^+). For **7**, the halfwave potential shifts to 562 ± 5 mV. Compound **5** exhibited only an irreversible oxidation at about 570 ± 20 mV at scan rates up to 2000 mV s^{-1}.

4. Conclusions

A series of novel bis-oligoprolinoyl–ferrocenes were synthesized successfully using the EDC/HOBt protocol. Inadvertantly, we obtained 1-oligoprolinoyl–1′-OBt–ferrocene derivatives as by-products. These compounds serve as stable synthons for ferrocenes derivatives carrying two different podant peptide chains, since the active OBt–ester can be exchanged readily for another peptide using the established procedures [7]. We are currently exploring this reaction further [10]. A single crystal X-ray structure determination of bis(prolinoyl methyester)ferrocene (**1a**) shows this molecule to be in the stable 1,3′-conformation in the solid state. This conformation prevents steric interactions of the substituents. NMR studies of **1**–**4** show that the two oligoproline residues on the Cp rings give rise to one set of signals. The chemical shift of the α-protons of the proline residues for compounds **1**–**7** are in a region of the spectrum characteristic for the peptide chain being in the helical polyproline-II conformation. Compounds **1**–**4** exhibit single reversible oxidation waves, which are dependent on the oligoproline chain length as was observed before for the monosubstituted Fc–oligoprolines. As the oligoproline chain grows in length and is able to adopt a stable polyproline-II helix, the Fc moiety becomes easier to oxidize.

5. Supplementary material

Crystallographic data for the structural analysis have been deposited with the Cambridge Crystallographic Data Centre, CCDC No. 155391. Copies of this information may be obtained free of charge from The Director, CCDC, 12 Union Road, Cambridge CB2 1EZ, UK (fax: +44-1233-336-033; e-mail: deposit@ccdc.cam.ac.uk or www: http://www.ccdc.cam.ac.uk).

Acknowledgements

This work was supported by grants from the National Science and Engineering Research Council of Canada (NSERC) and the Health Services Utilization and Research Commission of the Province of Saskatchewan (HSURC). We thank G.D. Enright for collection of the data set for **1a**.

References

[1] H.-B. Kraatz, D.M. Leek, A. Houmam, G.D. Enright, J. Lusztyk, D.D.M. Wayner, J. Organomet. Chem. 589 (1999) 38.
[2] (a) E. Gallopini, M.A. Fox, J. Am. Chem. Soc. 118 (1996) 2299;
(b) M.A. Fox, E. Gallopini, J. Am. Chem. Soc. 119 (1997) 5277.
[3] L. Lin, A. Berces, H.-B. Kraatz, J. Organomet. Chem. 556 (1998) 11.
[4] In acetonitrile, 0.1 M TBAP, glassy carbon, Ag | AgCl, vs. internal ferrocene/ferrocenium.
[5] (a) J.D. Schmitt, M.S.P. Sansom, I.D. Kerr, G.G. Lunt, R. Eisenthal, Biochemistry 36 (1997) 1115;
(b) W. Bauer, K. Polborn, W. Beck, J. Organomet. Chem. 579 (1999) 269;
(c) E. Manoury, J.S. Fossey, H. Aït-Haddou, J.-C. Daran, G.G.A. Balavoine, Organometallics 19 (2000) 3736;
(d) P. Saweczko, H.B. Kraatz, Coord. Chem. Rev. 190-192 (1999) 185.
[6] (a) A. Nomoto, T. Moriuchi, S. Yamazaki, A. Ogawa, T. Hirao, Chem. Commun. (1998) 1963;
(b) T. Moriuchi, A. Nomoto, K. Yoshida, T. Hirao, J. Organomet. Chem. 589 (1999) 50;
(c) T. Moriuchi, A. Nomoto, K. Yoshida, A. Ogawa, T. Hirao, J. Am. Chem. Soc. 123 (2001) 68–75.
[7] M. Bodanszky, A. Bodanszky, The Practice of Peptide Synthesis, 1st ed., Springer-Verlag, Berlin, 1984.
[8] SHELXTL, Version 5, Siemens Energy and Automation Inc., 1994.
[9] Southhamptom Electrochemistry Group, Instumental Methods in Electrochemistry, Wiley, New York, 1985.
[10] Y. Xu, H.B. Kraatz, Tetrahedron Lett. 42 (2001) 2601–2603.